

R-09-020-015

UNITED STATES
DEPARTMENT OF THE INTERIOR
GEOLOGICAL SURVEY

INTERAGENCY REPORT NASA-122

GRIDDING OF NEAR VERTICAL
UNRECTIFIED SPACE PHOTOGRAPHS*

by

GPO PRICE \$ _____

CFSTI PRICE(S) \$ _____

Richard H. Rapp**

and

Hard copy (HC) 3-00

William H. Sprinsky**

Microfiche (MF) .65

June 1968

ff 653 July 65

Prepared by the Geological Survey
for the National Aeronautics and
Space Administration (NASA)

*Work performed under NASA Contract No. 14-08-0001-10666, Task 160-75-01-30-10
**Ohio State University, Columbus, Ohio

FACILITY FORM 602	N 68-27573	
	(ACCESSION NUMBER)	(THRU)
	45	1
	(PAGES)	(CODE)
	CR 95226	14
	(NASA CR OR TMX OR AD NUMBER)	(CATEGORY)

FOREWORD

This report was prepared by Richard H. Rapp, Associate Professor and Captain William H. Sprinsky, Research Assistant, Department of Geodetic Science, The Ohio State University. This research was sponsored by the U. S. Department of the Interior, Geological Survey under contract No. 14-08-0001-10666, The Ohio State University Research Foundation Project 2336.

ABSTRACT

The gridding of unrectified space photographs is described from two viewpoints. The first considers a mathematical model relating points on the surface of the earth to their image on a space photograph. An adjustment procedure is then derived for near vertical photographs. This procedure would allow for the determination of the location and orientation of the space photograph if ground control and approximate values of the parameters are available. The second viewpoint considers that, for many space photographs, we do not know to a sufficient accuracy the location and orientation parameters of the photograph. We then perform a least squares surface fit of the ground control to the coordinates on the photograph. Either viewpoint yields equations that may be used to place grids on the space photographs. Future work is suggested.

TABLE OF CONTENTS

	<u>Page</u>
1. INTRODUCTION.	1
2. THE SURFACE - SPACE PHOTOGRAPH RELATIONSHIP.	2
2.1 The Vertical Photograph.	2
2.2 The Non-Vertical Photograph.	9
2.3 The Effect of Small Tilts Only.	13
3. THE ADJUSTMENT PROCEDURE FOR A NEAR VERTICAL PHOTOGRAPH.	14
3.1 Introduction.	14
3.2 The Adjustment System.	15
3.3 The Partial Derivatives.	16
3.31 The A Matrix.	16
3.32 The B Matrix.	20
3.4 Discussion of the Adjustment System.	20
3.5 Final Result of the Generalized Adjustment Scheme.	22
4. AN ALTERNATE SURFACE - PHOTOGRAPH RELATIONSHIP.	23
4.1 Introduction.	23
4.2 Approximate Transformation From Surface to Photograph Coordinates.	24
4.3 Limitations of the Approximate Method.	24
5. GRIDDING PROCEDURES AND THE USE OF MAP PROJECTIONS.	25
5.1 Introduction - Geographic Gridding.	25
5.2 The Height of the Grid.	26
5.3 Gridding in a Specified Map Projection.	27
5.31 Applications of the Universal Transverse Mercator (UTM) Projection.	28
6. RESULTS OF TEST GRIDDING.	30
6.1 Introduction.	30
6.2 Photograph No. One.	32
6.3 Photograph No. Two.	34
6.4 Photograph No. Three.	40
7. DISCUSSION AND CONCLUSION.	43
7.1 Summary.	43
7.2 Conclusion.	43
7.3 Future Work.	44
REFERENCES.	46

1. Introduction

The gridding of satellite photographs is an important tool in obtaining information from a photograph, or some image, recorded in space. The obvious reason is that, in general, for the information portrayed in the image to be of use, we generally need to know the location on the earth of that information.

In recent years the most prolific information in this area has come from the various weather satellites in which a television image is created. For the interpretation of the cloud structure, it was necessary to create techniques for the gridding of the images. Much analysis in this area may be found in the reports and papers of Fujita (1963, 1964, 1965), Bonner (1965), Widger (1965), Grenard (1963) and others. The procedures developed in this area generally required the sub-satellite point in latitude and longitude, the orientation of the spin axis (to which the camera direction was closely associated), and the height of the satellite. In addition this data was regarded as exactly known, with the effect of errors in the input data being estimated on the accuracy of the constructed grid. Additionally the earth is assumed to be a sphere which is sufficient for the accuracy required for the problem.

For the purpose of this report the above methods do not meet our requirements as we do not wish to assume that we know the exact coordinates of the location of the taking camera, nor that the earth is a sphere. On the other hand, we will be assuming at a later stage that the photographs that we will attempt to grid are near vertical photographs.

Other work in the area of gridding of space photographs may be found in the works of Dumitrescu (1966, 1967). He forms analytical and graphical methods of placing grids on photographs where we know various parameters required in the location and orientation of the taking camera. Unfortunately it is the rare satellite photograph for which such information is available and thus the techniques presented by Dumitrescu are not applicable.

We now come to the purpose of this report. This is to develop methods for the gridding of unrectified space photographs in two contexts: 1) When the approximate location and orientation of the taking camera is specified. Such a solution would seek to utilize available ground control to obtain the gridding of the photograph along with the best estimates for the location or orientation of the camera; 2) No data is available on the location or orientation of the camera. Such a method should try to form some correspondence between the coordinates measured on the photograph and the latitude and longitude lines.

The theory will be worked out for the two above situations. Because of lack of data, it will be possible to carry out the actual gridding only for the second method. This gridding will be in latitude and longitude lines, and in some cases in terms of some particular coordinates of a given map projection. This latter gridding is of interest when we might want to work with respect to a rectangular coordinate system, such as the UTM (Universal Transverse Mercator Projection). However it should be realized that the rectangular axes of such a projection will not be orthogonal, nor straight when represented on the unrectified space photographs.

2. The Surface - Space Photograph Relationship

2.1 The Vertical Photograph

We seek to relate a given point on the surface of the earth specified by its latitude, ϕ_p , longitude λ_p , and its height, H_p , above some reference ellipsoid, to x and y coordinates on the photographic plate obtained from a satellite borne camera. This is accomplished by first considering the transformation of the ground point to a vertical photograph and then modify the relationship to consider that the photograph is only slightly tilted.

First we consider the geometry of a vertical photograph as presented in Figure 1.

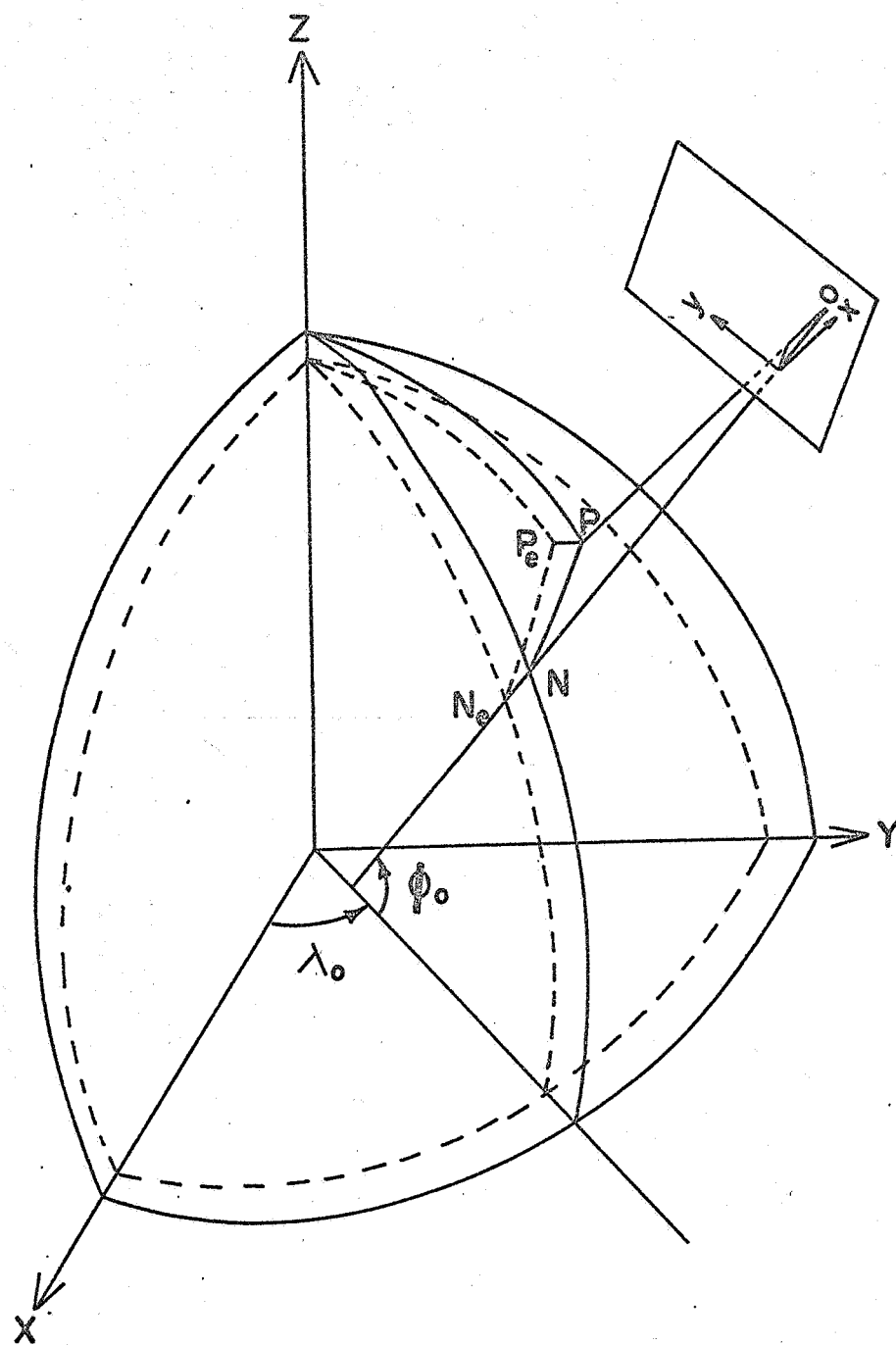


Figure 1

Geometry of a Vertical Space Photograph

In this figure we have the following quantities:

- O Interior node of taking camera
- $N_0 NO$ Line normal to ellipsoid (dotted lines) through O, and perpendicular to the plane of the photograph. N is the location of N_0 as viewed on the actual surface from O
- x, y fiducial axes established in the photograph defined so that y is in the intersection of the plane containing the interior node and the meridian passing through N_0 . x is perpendicular to y, considered positive east.
- Op line connecting an arbitrary point P, on the surface of the earth, with O
- $P_0 P$ normal to ellipsoid passing through P
- φ_0, λ_0 geodetic latitude and longitude of point N_0 ; φ_0, λ_0 are generally referred to as the footpoint latitude and longitude.
- φ_p, λ_p geodetic latitude and longitude of point P_0

The normal section azimuth (α_{12}) from N_0 to P_0 would be given by the following equations [Robbins, 1962]:

$$(1) \quad \cot \alpha_{12} = \cot \alpha_{N_0 P_0} = \frac{\cos \varphi_0 \tan \psi - \sin \varphi_0 \cos (\lambda_p - \lambda_0)}{\sin (\lambda_p - \lambda_0)}$$

where:

$$\tan \psi = (1 - e^2) \tan \varphi_p + \frac{e^2 N_0 \sin \varphi_0}{N_{p_e} \cos \varphi_p}$$

where:

N_0 = radius of curvature in the prime vertical at N_0

N_p = radius of curvature in the prime vertical at P_0

In general:

$$(3) \quad N = \frac{a}{(1 - e^2 \sin^2 \varphi)^{\frac{1}{2}}}$$

where a is the equatorial radius of the reference ellipsoid and e is the

eccentricity of this ellipsoid.

If we let H_m be the height of point N_e above the ellipsoid (that is the distance $N_e N$), the space rectangular coordinates of N_e are:

$$(4) \quad X_0 = (N_0 + H_m) \cos \varphi_0 \cos \lambda_0$$

$$(5) \quad Y_0 = (N_0 + H_m) \cos \varphi_0 \sin \lambda_0$$

$$(6) \quad Z_0 = (N_0 (1 - e^2) + H_m) \sin \varphi_0$$

For the arbitrary point P we have, similarly

$$(7) \quad X_p = (N_p + H_p) \cos \varphi_p \cos \lambda_p$$

$$(8) \quad Y_p = (N_p + H_p) \cos \varphi_p \sin \lambda_p$$

$$(9) \quad Z_p = (N_p (1 - e^2) + H_p) \sin \varphi_p$$

where H_p is the height of P above the ellipsoid. If we designate the chord between N and P as Q we may write:

$$(10) \quad Q = \left[(X_p - X_0)^2 + (Y_p - Y_0)^2 + (Z_p - Z_0)^2 \right]^{\frac{1}{2}}$$

A vector, \vec{v} , from N to P, would be:

$$(11) \quad \vec{v} = \frac{(X_p - X_0)}{Q} \vec{i} + \frac{(Y_p - Y_0)}{Q} \vec{j} + \frac{(Z_p - Z_0)}{Q} \vec{k}$$

where \vec{i} , \vec{j} , and \vec{k} are unit vectors along the coordinates axes, X, Y, Z, respectively. Similarly, a unit vector along the normal from N to O would be written:

$$(12) \quad \vec{u} = \cos \varphi_0 \cos \lambda_0 \vec{i} + \cos \varphi_0 \sin \lambda_0 \vec{j} + \sin \varphi_0 \vec{k}$$

In order to see how the vectors, \vec{v} and \vec{u} may be used consider Figure 2 and Figure 3.

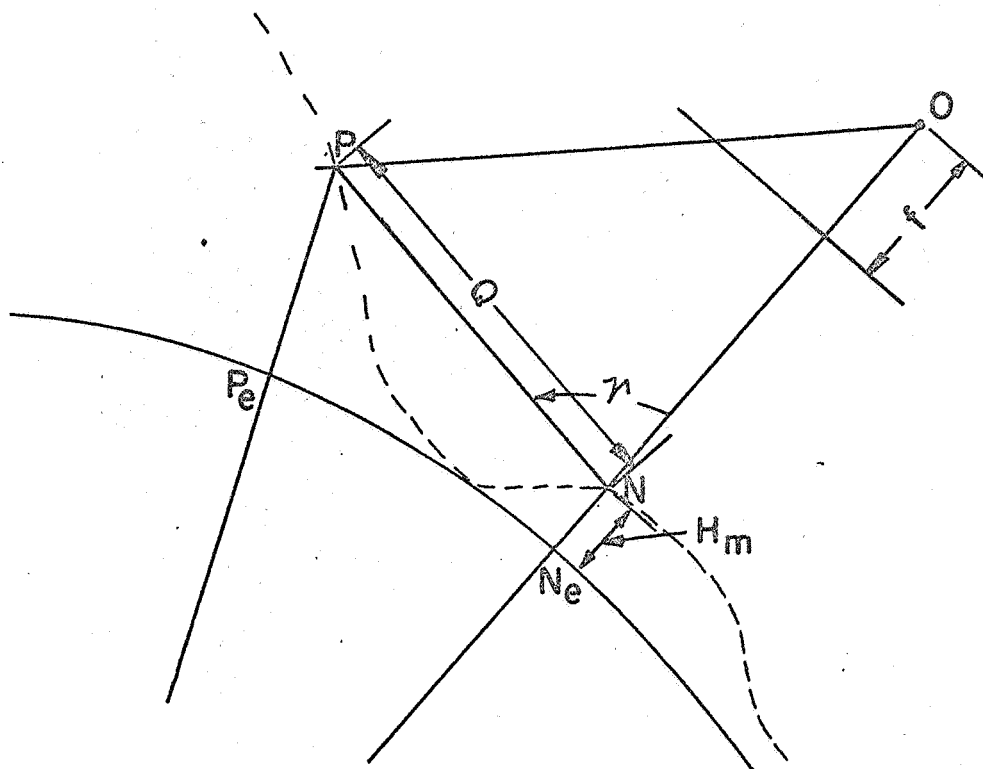


Figure 2

Section Containing Surface and Photograph

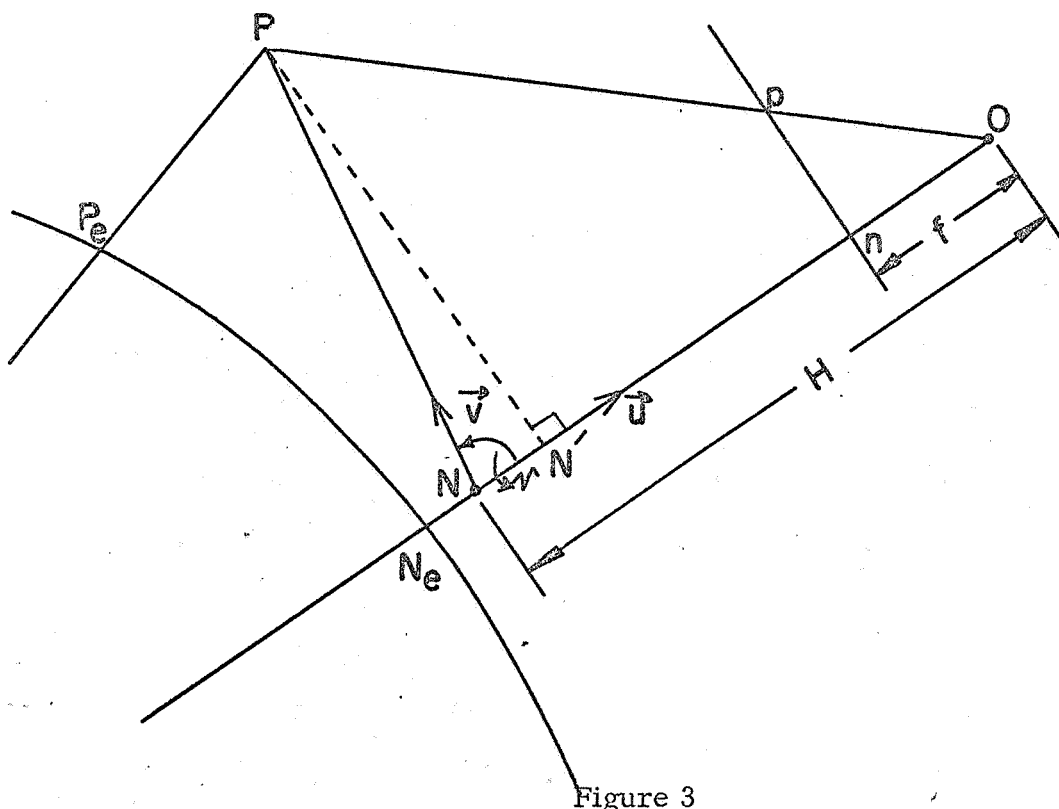


Figure 3

Location of Point N'

This figure represents a section containing the interior node of the taking camera, the arbitrary point P and the subpoint N, both located on the physical surface of the earth. Angle γ is the angle PNO which may be found from the dot product of the two unit vectors along NP (i.e. \vec{v}) and NO (i.e. \vec{u}).

Thus:

$$(13) \quad \cos \gamma = \vec{v} \cdot \vec{u} = \frac{X_p - X_o}{Q} \cos \varphi_o \cos \lambda_o + \frac{Y_p - Y_o}{Q} \cos \varphi_o \sin \lambda_o + \frac{Z_p - Z_o}{Q} \sin \varphi_o$$

In order to consider the location of point P on the photograph, p, we consider Figure 3. In this figure, f represents the focal length of the camera, H is the height of O above the ellipsoid, and N' is an auxiliary point located on a line perpendicular to N_eO, passing through P, and n is the intersection of the photograph with the line N_eO.

From the figure we have:

$$(14) \quad NN' = Q \cos \gamma$$

$$(15) \quad PN' = Q \sin \gamma$$

From similar triangles (Opn and OPN') we have:

$$(16) \quad \frac{PN'}{H - Q \cos \gamma} = \frac{\overline{pn}}{f}$$

So that:

$$(17) \quad \overline{pn} = \frac{fQ \sin \gamma}{H - Q \cos \gamma}$$

where \overline{pn} is the distance in the plane of the photograph between p and n.

We are now able to compute the coordinates of P in the photograph by finding the components of \overline{pn} in the x and y directions. Looking down from O the photograph would be seen as in Figure 4.

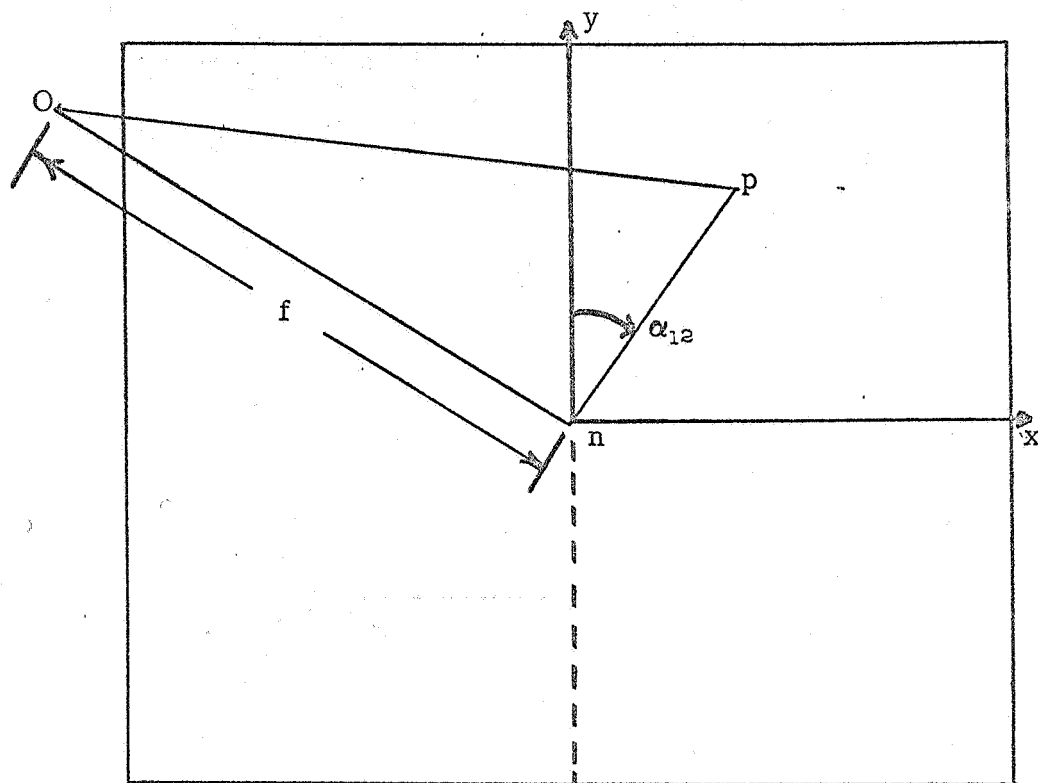


Figure 4

Photograph as Viewed From Above

Since y is defined in the direction of the meridian through the footpoint, N_0 , the azimuth between N and P in the ground will be the same as between n and p in the photograph. Thus:

$$(18) \quad \begin{aligned} x &= \overline{pn} \sin \alpha_{12} \\ y &= \overline{pn} \cos \alpha_{12} \end{aligned}$$

or

$$(19) \quad \begin{aligned} x &= \frac{fQ \sin \gamma \sin \alpha_{12}}{H - Q \cos \gamma} \\ y &= \frac{fQ \sin \gamma \cos \alpha_{12}}{H - Q \cos \gamma} \end{aligned}$$

For future reference we define:

$$\begin{aligned} c &= \frac{fQ \sin \gamma \sin \alpha_{12}}{H - Q \cos \gamma} \\ c_2 &= \frac{fQ \sin \gamma \cos \alpha_{12}}{H - Q \cos \gamma} \end{aligned}$$

Equation (19) could be used for the location of ground points on a space photograph if the photograph were vertical. In this context a vertical photograph is one where the nadir point n is identical with the point at the center of the photograph. However, this is far from the true situation so that we must now consider the effect of a non-vertical photograph on the photo coordinates.

2.2 The Non-Vertical Photograph

The non-vertical photograph problem is considered by attempting to apply three rotations to or from a vertical photograph. The rotations are designated Φ , ω , and κ .

We now consider first the effect of a Kappa (κ) rotation. We designate y''' , x''' , as the actual fiducial axes in the photograph. In general the orientation will differ from the ideal x, y orientation originally established in section 2.1. For this purpose κ is defined as the angle between the y''' axis and the image of the meridian, (designating geodetic north) through N_0 , on the photograph. This angle is measured in a positive direction, clockwise, from the y''' axis to the meridian image. If we designate the system rotated from the x''', y''' system as x'', y'' , we may see by applying a rotation about the z''' axis shown in Figure 5, that:

$$(20) \quad \begin{aligned} x'' &= x''' \cos \kappa - y''' \sin \kappa \\ y'' &= y''' \cos \kappa + x''' \sin \kappa \end{aligned}$$

Now we must consider the tilt of the photograph with respect to the vertical situation. First we consider the effect of a ϕ tilt or rotation, where ϕ is the angle, measured at O , between a line perpendicular to the $y''x''$ plane and the $y'x'$ plane measured in the $y''x''$ plane. The geometry of the situation is shown in Figure 6.

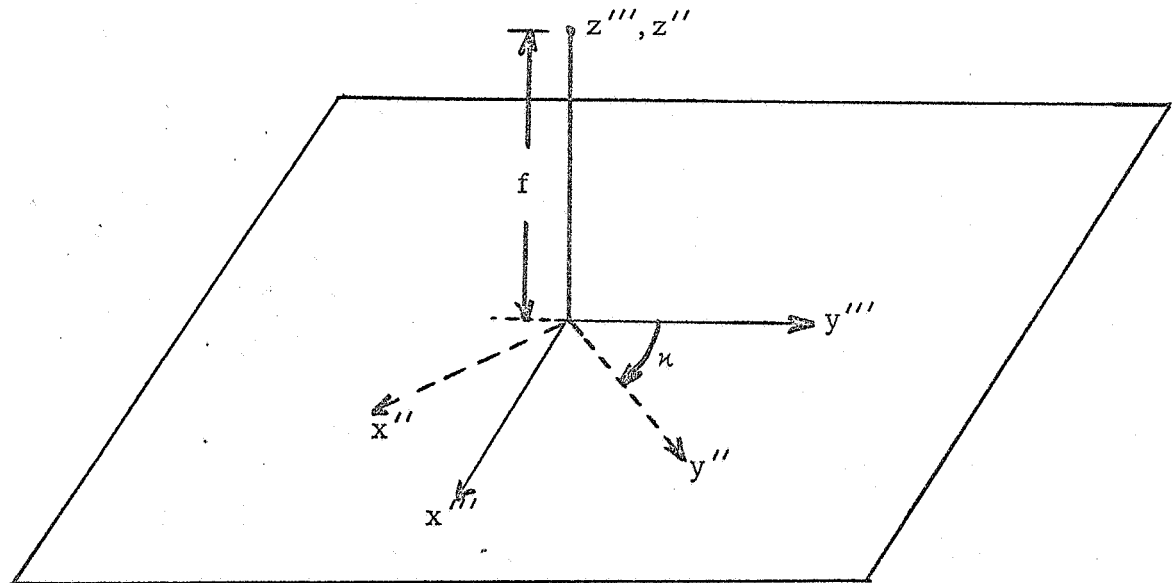


Figure 5
The Kappa Rotation

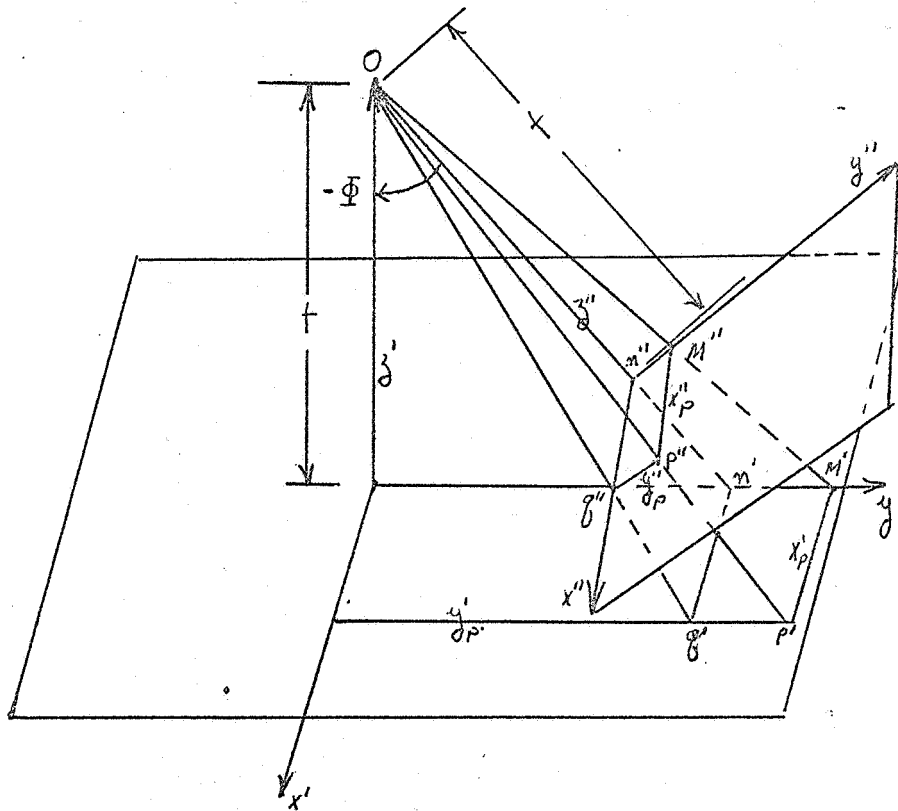


Figure 6

The Phi (Φ) Rotation

In this figure the $x'y'$ plane represents a plane vertical with respect to the y' orientation. p'' is a point on the x'', y'' plane, whose image on the $x'y'$ plane is p' . The coordinates of p' are designated as x' and y' . From triangle OAM' we have:

$$(21) \quad y' = f \tan \left(\Phi + \tan^{-1} \frac{y''}{f} \right)$$

which may be expanded as the tangent of the sum of two angles to yield:

$$(22) \quad y' = \frac{f \tan \Phi + y''}{1 - \frac{\tan \Phi y''}{f}}$$

From the similar triangle $On''q''$ and $On'q'$ we have:

$$x' = \left(\frac{x''}{f} \right) \left(\frac{f}{\cos \Phi} \right)$$

so that:

$$(23) \quad x' = \frac{x''}{\cos \Phi}$$

We now complete the rotation of the original non-vertical photograph by the angle ω which represents the third orientation angle. This is the angle between the perpendicular to the $y'x'$ plane and the yx plane measured in the $x'x$ plane. Reasoning similar to that for the Φ rotation yields the coordinates on a vertical photograph as:

$$(24) \quad x = \frac{f \tan \omega + x'}{1 - \frac{\tan \omega x'}{f}}$$

$$(25) \quad y = \frac{y'}{\cos \omega}$$

In order to transform completely from the coordinates on a tilted photograph to a vertical photograph oriented with the y axis in the direction of the meridian through the point N_0 it would be necessary to substitute equations (20) into equations (22) and (23), and then substitute the results into equations (24) and (25). The result will be complicated but will represent the geometry of the arbitrarily oriented non-vertical photograph with respect to an oriented vertical photograph.

2.3 The Effect of Small Tilts Only

The general aim of this report is to consider photographs of the near vertical type. Thus we may assume that ϕ and ω are small. Then we may take:

$$\begin{aligned} \sin \phi &\approx \tan \phi \approx \phi \\ (26) \quad \sin \omega &\approx \tan \omega \approx \omega \\ \cos \phi &\approx \cos \omega \approx 1 \end{aligned}$$

Then equations (22) and (23) may be written as

$$\begin{aligned} (27) \quad y' &= f\phi + y'' \\ x' &= x'' \end{aligned}$$

and equations (24) and (25) become

$$\begin{aligned} (28) \quad x &= f\omega + x' \\ y &= y' \end{aligned}$$

Thus we can write for a near vertical photograph:

$$\begin{aligned} (29) \quad y &= f\phi + y'' = f\phi + y''' \cos \kappa + x''' \sin \kappa \\ x &= f\omega + x'' = f\omega + x''' \cos \kappa - y''' \sin \kappa \end{aligned}$$

In this equation set, $f\phi$ and $f\omega$ may be interpreted as small shifts in the origin from that on the original photograph to one on the vertical photograph, while the remaining parts of the equation represent the rotation required for proper orientation of the coordinate axes.

If we now compare equations (29) with the equations (19) derived on the true vertical assumptions we have:

$$\begin{aligned}
 (30) \quad & \frac{fQ \sin \gamma \sin \alpha_{12}}{H - Q \cos \gamma} - f\omega - x''' \cos \kappa + y''' \sin \kappa = 0 \\
 & \frac{fQ \sin \gamma \cos \alpha_{12}}{H - Q \cos \gamma} - f\phi - y''' \cos \kappa - x''' \sin \kappa = 0
 \end{aligned}$$

If all theory is correct equations (30) should be exactly zero. However because of the approximations made with respect to the angles ϕ and ω , (30) will only be approximately zero. For our purposes, they are sufficient and will form the mathematical structure for further treatment of the problem.

If we would desire to compute the coordinates in the near-vertical photograph from ground points we could use (30) to write:

$$\begin{aligned}
 y''' &= -(x - f\omega) \sin \kappa + (y - f\phi) \cos \kappa \\
 x''' &= (x - f\omega) \cos \kappa + (y - f\phi) \sin \kappa
 \end{aligned}$$

where x, y are given in equations (19).

3. The Adjustment Procedure For a Near-Vertical Photograph

3.1 Introduction

In order to compute the coordinates of an arbitrary point on the space photograph using the previously derived equations, it is necessary to specify six parameters that describe the location and orientation of the space camera. These are ϕ_0 , λ_0 , the subsatellite point, H , the height of the camera, ϕ , ω , and κ . We assume that the focal length, f , of the camera is known.

At this stage in the technology it is not feasible to accurately determine these parameters. It may only be done after the photograph has been taken and then only when approximate values of ϕ_0 , λ_0 , H , ϕ , ω , and κ are available. In addition, for the present study the assumption of near vertical photography must exist.

We then proceed to an adjustment system where we combine the approximate estimates of the parameters with data observed in the photograph in conjunction with ground control information, to obtain the best

estimates of the parameters φ_0 , λ_0 , H , Φ , ω , and κ . Once this is done we could take any point on the surface of the earth and compute its x, y coordinate in the photograph. By properly specifying the coordinate on the surface we may construct a grid on the photograph.

3.2 The Adjustment System

Given a function F which is a function of parameter x_j , and observations l_b , we may write:

$$(32) \quad F(x_1, x_2, \dots, x_n, l_1, l_2, \dots, l_b) = 0$$

If we linearize this equation and denote the corrections to the approximate parameters as a column matrix X , and corrections to the observed quantities V , also a column matrix, we may write [Schmid and Schmid, 1965]:

$$(33) \quad AX + BV + W = 0$$

where W is a column matrix called a misclosure matrix. W is equal to the value of the function in equation (32) evaluated with the observed quantities and the approximate values of the parameters. In our particular case the parameters are corrections to φ_0 , λ_0 , H , Φ , ω , κ while the observations would be the measured plate coordinates in the near-vertical photograph.

The length of the column matrix W will depend on the number of observed points. Since there are two coordinates, x''' and y''' , for each point, there will be $2n$ elements in W where n is the number of measured points in the photograph.

In our case matrix A would be composed of $2n$ rows and six columns. Each element of A represents the partial derivative of the function F with respect to the particular parameter considered (i.e. φ_0 , λ_0 , H , Φ , ω , or κ). Matrix B will be composed of $2n$ rows and $2n$ columns where each element of B represents the partial derivative of the function F with respect to each of the original observations.

If we let P_x be a weight matrix for the parameters to be found, and P_l

be the weight matrix of the observation, the least squares solution for the parameters will be: [Schmid and Schmid, 1965]

$$(34) \quad X = -P_x^{-1} A' \left[AP_x^{-1} A' + BP_\ell^{-1} B' \right] W$$

If we do not desire to weight the parameters, we may set $P_x = 0$ and (34) becomes:

$$(35) \quad X = -(A'M^{-1}A)^{-1} (A'M^{-1}W)$$

where

$$M = BP_\ell^{-1}B'$$

3.3 The Parital Derivatives

3.31 The A Matrix

At this point we must differentiate the specific functional relationships in the form of equation (32) in order to obtain the A and the B matrices. From equation (30) we may indicate the functional relationship as:

$$(35) \quad \begin{aligned} F_A (\varphi_0, \lambda_0, H, \Phi, \omega, \kappa, x''', y''') &= 0 \\ F_B (\varphi_0, \lambda_0, H, \Phi, \omega, \kappa, x''', y''') &= 0 \end{aligned}$$

where the first equation of (35) is associated with the first equation of (30) and in a similar fashion, the second equation. The first six values listed in the functions are the parameters whose best values are to be estimated while x''' and y''' represent the observations.

For each observation, there will be a row in the A matrix composed of six partial derivatives as follows:

$$(36) \quad \begin{aligned} &\frac{\partial F_A}{\partial \varphi_0}, \frac{\partial F_A}{\partial \lambda_0}, \frac{\partial F_A}{\partial H}, \frac{\partial F_A}{\partial \Phi}, \frac{\partial F_A}{\partial \omega}, \frac{\partial F_A}{\partial \kappa} \\ &\frac{\partial F_B}{\partial \varphi_0}, \frac{\partial F_B}{\partial \lambda_0}, \frac{\partial F_B}{\partial H}, \frac{\partial F_B}{\partial \Phi}, \frac{\partial F_A}{\partial \omega}, \frac{\partial F_A}{\partial \kappa} \end{aligned}$$

PRECEDING PAGE BLANK NOT FILMED.

$$H \frac{\partial F_B}{\partial H} = \frac{-c_2 H}{H - Q \cos \gamma}$$

$$\frac{\partial F_A}{\partial \Phi} = 0$$

$$\frac{\partial F_B}{\partial \Phi} = -f$$

$$\frac{\partial F_A}{\partial \omega} = -f$$

$$\frac{\partial F_B}{\partial \omega} = 0$$

$$\frac{\partial F_A}{\partial \kappa} = x''' \sin \kappa + y''' \cos \kappa$$

$$\frac{\partial F_B}{\partial \kappa} = -x''' \cos \kappa + y''' \sin \kappa$$

where:

$$D = - \frac{(X_p - X_0) S_1 + (Y_p - Y_0) S_2 + (Z_p - Z_0) S_3}{Q}$$

$$J = \frac{(X_p - X_0) Y_0 - (Y_p - Y_0) X_0}{Q}$$

$$G = \frac{\sin^2 \alpha_{12}}{\sin (\lambda_p - \lambda_0)} \cdot \left(\sin \varphi_0 \tan \Psi + \cos \varphi_0 (\cos (\lambda_p - \lambda_0) - S_4) \right)$$

$$E = \frac{1}{Q \sin \gamma} \left[D \cos \gamma + (X_p - X_0) \sin \varphi_0 \cos \lambda_0 + S_1 \cos \varphi_0 \cos \lambda_0 \right. \\ \left. + (Y_p - Y_0) \sin \varphi_0 \sin \lambda_0 + S_2 \cos \varphi_0 \sin \lambda_0 - (Z_p - Z_0) \cos \varphi_0 \right. \\ \left. + S_3 \sin \varphi_0 \right]$$

$$K = \frac{1}{Q \sin \gamma} \left[\cos \gamma - (X_p - 2X_0) \cos \varphi_0 \sin \lambda_0 + Y_p \cos \varphi_0 \cos \lambda_0 \right]$$

$$L = \frac{\sin^2 \alpha_{12}}{\sin^2 (\lambda_p - \lambda_0)} (-\cos \varphi_0 \tan \Psi \cos (\lambda_p - \lambda_0) + \sin \varphi_0)$$

where:

$$S_1 = - (N_0 + H_m) \sin \varphi_0 \cos \lambda_0 + \frac{e^2 M_0 \sin 2\varphi_0}{2 (1 - e^2)} \cos \varphi_0 \cos \lambda_0$$

$$S_2 = - (N_0 + H_m) \sin \varphi_0 \sin \lambda_0 + \frac{e^2 M_0 \sin 2\varphi_0}{2 (1 - e^2)} \cos \varphi_0 \sin \lambda_0$$

$$S_3 = (N_0 (1 - e^2) + H_m) \cos \varphi_0 + \frac{e^2 M_0 \sin 2\varphi_0}{2} \sin \varphi_0$$

$$S_4 = \frac{e^2 N_0 \cos \varphi_0 + \left(\frac{e^4 M_0 \sin 2\varphi_0}{2 (1 - e^2)} \right) \sin \varphi_0}{N_p \sin \varphi_0}$$

where:

$$M_0 = \frac{a (1 - e^2)}{(1 - e^2 \sin^2 \varphi_0)^{\frac{3}{2}}}, \quad N_{\{P\}} = \frac{a}{(1 - e^2 \sin^2 \varphi_{\{P\}})^{\frac{1}{2}}}$$

The coefficient of H in the parameter set has been taken here as the coefficient of the unknown dH/H. This is done so that all unknowns will be of the same size numerically.

Needless to say these equations are complex and their hand evaluation would be too laborious for anything but test computations. However once they have been programmed for a computer their complexity would only be apparent in the computer time required for the solution.

For this reason no attempt at simplification through approximations was made. It should be noted that once the approximate parameters are specified and a certain control point, visible in the photograph identified, all coefficients given may be computed.

3.32 The B Matrix

Considering equation (35) with equation (30), and recalling that the observations are x''' and y''' , we have:

$$(38) \quad \begin{aligned} \frac{\partial F_A}{\partial x'''} &= -\cos \kappa ; & \frac{\partial F_B}{\partial x'''} &= -\sin \kappa \\ \frac{\partial F_A}{\partial y'''} &= \sin \kappa ; & \frac{\partial F_B}{\partial y'''} &= -\cos \kappa \end{aligned}$$

3.4 Discussion of the Adjustment System

Sections 3.1, 3.2, and 3.3 have presented the equations required for the adjustment of space photograph data in order to obtain the location and orientation of the taking camera. Since there are six parameter unknowns, a minimum of three control points on a photograph are required. However, we always desire more observations than the minimum required. Ideally we should have control spread throughout the photograph.

In order to apply the adjustment presented here we need the approximate values of φ_0 , λ_0 , H , Φ , ω , and κ . Assuming a near vertical photograph, we could compute the value of φ_0 , λ_0 , and H from the orbital elements of the satellite, if we knew the exact time of exposure. These values should be

accurate enough for approximate entry into the solution if such a time is known to within approximately one-half second--perhaps one second is sufficient. Since we assume the photograph near vertical, the starting values for ϕ and ω may be zero. However, the value of κ may be between 0° and 360° so that we must be able to compute an approximate value for it, starting from data available in the photograph.

In figure 7, a sketch is shown with the orientation of the fiducial axes x''' , y''' of the actual photograph, and the system orientated with its y axis pointing north, aligned with the meridian passing through the subsatellite point.

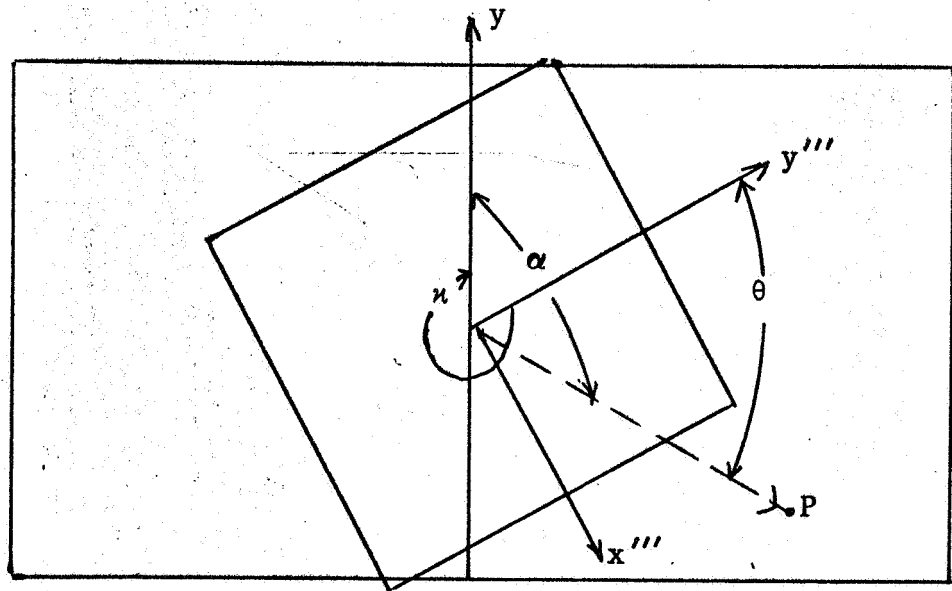


Figure 7

Alignment of Fiducial Axes

Consider some known point P on the photograph and on the surface of the earth. Let α be the azimuth from the subsatellite point to point P measured on the ellipsoid (actually only an approximation to its azimuth is required); let θ be the angle between the y''' axis and the line on the photograph connecting the image of the subsatellite point and the P point on the photograph; let κ be the angle from the y''' axis to the y axis measured positive in a

clockwise direction. Then from the figure we have:

$$(39) \quad \kappa = 360^\circ - (\alpha^\circ - \theta^\circ)$$

Using this procedure, an approximate value of κ is obtained.

We must also consider the assignment of weights for the P_x and P_s matrices. The weight in P_x and P_s may be determined from

$$(40) \quad P = \frac{1}{m^2}$$

where m is the "a priori" estimate of the standard error of the approximate value of φ_0 , λ_0 , H_0 , Φ , ω , and κ , or the standard error of the observations of x''' and y''' in the measurement system of the photographic plate.

The assignment of the "a priori" standard errors is difficult. It will depend on exactly how the parameters were determined. In some cases it may be that some of the parameters may be poorly determined by the adjustment procedure. It may then be necessary to obtain as accurate estimates as possible causing a high weight to be assigned to the parameters. Through the assignment of high weights to the parameters it is also possible to contain certain of the parameters to specified values.

Some testing was carried out in performing the adjustment described here. From fictitious situations the equations derived were shown to be apparently valid. The sample adjustments showed that the results were highly sensitive to the approximate input parameters and to the "a priori" weights assigned. It was also apparent that several of the parameters are highly correlated. For example there is high correlation between φ_0 and Φ , and λ_0 and ω .

3.5 Final Result of the Generalized Adjustment Scheme

Assuming that we have the proper input data and the adjustment is successful, we would obtain best estimates for φ_0 , λ_0 , H_0 , Φ , ω , κ . Thus

if we were given a value for x''' and y''' on the photograph of some point we theoretically could go back to equation (30) to find, ultimately the ground coordinates φ_p, λ_p if H_p were known.

However, for the construction of grids on the photograph it is more important that we are able to go from a ground point to a point on the photograph. This may be done, once the location and orientation of the photograph have been obtained, through equations (31) and (19).

The actual gridding procedures will be described in a later section.

4. An Alternate Surface - Photograph Relationship

4.1 Introduction

Although the discussions carried out in sections 2 and 3 are sufficient to solve the gridding problem if we know the input data, it was found that with existing space photographs, such as produced by the Gemini experiment, such information does not exist. Thus we were not able to apply the method outlined in sections 2 and 3 because we were unable to obtain any data on the location (other than an approximate area location) or the orientation of the photograph. The reason for this is that the photographic mission of Gemini did not require near vertical photography nor the timing of the photographic exposure. We are thus left with the prospect of having the Gemini photography but without the ability to grid it unless extensive photo by photo analysis is carried out, by rectification, to obtain the approximate value of the unknown parameters.

In an attempt to circumvent this problem an attempt was made to develop a numerical transformation between the surface points and the corresponding points in the photograph. This approach does not require the six location and orientation parameters of the camera and consequently it has limited application as will be seen later in actual tests.

4.2 Approximate Transformation From Surface to Photograph Coordinates

We assume that we may represent x''' , y''' of some point as a mixed polynomial in the latitude, φ , and the longitude λ , of the point on the surface viewed by the photograph. Specifically we take:

$$\begin{aligned}
 x''' - x_0''' &= a_1 (\varphi - \varphi_0) + a_2 (\lambda - \lambda_0) + a_3 (\varphi - \varphi_0)^2 + a_4 (\lambda - \lambda_0)^2 \\
 &\quad + a_5 (\varphi - \varphi_0)(\lambda - \lambda_0) \\
 (41) \quad y''' - y_0''' &= b_1 (\varphi - \varphi_0) + b_2 (\lambda - \lambda_0) + b_3 (\varphi - \varphi_0)^2 + b_4 (\lambda - \lambda_0)^2 \\
 &\quad + b_5 (\varphi - \varphi_0)(\lambda - \lambda_0)
 \end{aligned}$$

If we let $p = \varphi - \varphi_0$ and $l = \lambda - \lambda_0$ these equations may be more compactly written as:

$$\begin{aligned}
 x''' - x_0''' &= a_1 p + a_2 l + a_3 p^2 + a_4 l^2 + a_5 pl \\
 (42) \quad y''' - y_0''' &= b_1 p + b_2 l + b_3 p^2 + b_4 l^2 + b_5 pl
 \end{aligned}$$

The value of x_0''' , y_0''' , φ_0 , and λ_0 are the measured and ground coordinates of some point near the center of the photograph. It is used as a reference origin for convenience.

The transformation is complete if we find the a and b coefficients. This may be done assuming we have a minimum of six known points. One of these points will act as the reference origin while the remaining five points are used to solve for the a and b values. We will generally have more than six control points so that a least squares solution is required. This solution carried out for equation (42) by specifying that the sum of the squares of the corrections to $x''' - x_0'''$ will be a minimum; and separately for the second equation in (42), we specify that the sum of the squares of the corrections to $y''' - y_0'''$ will be a minimum. Thus, providing sufficient control is available, we will be able to determine the a and b values and thus be able to transform any given φ and λ to a coordinate x''' and y''' on the photo.

4.3 Limitations of the Approximate Method

The method described in this section is fundamentally representative of a surface to plane transformation. It may be justified as an approximation of

the projective transformation from one plane to another where we would be assuming that the surface of the earth in the small area of the photographic image may be approximated as a plane. The higher order terms and cross product terms in (42) may absorb much of the theoretical transformation errors but certain errors must be in this model. This effect would be evident as part of the residuals obtained from the adjustment procedure.

In combination with the neglect of unknown terms in equation (42) we must consider the fitting of the ϕ, λ coordinates to the x, y system for extrapolation purposes. We must be careful in this situation because it is possible, in fact probable, that the transformation fitted to known coordinates will not yield a meaningful transformation in an area outside the known point area.

5. Gridding Procedures and the Use of Map Projections

5.1 Introduction - Geographic Gridding

We now desire to place a grid on a given photograph. This grid may be composed of the images of the meridians and parallels, or may be the images of the coordinate lines of some specified map projection. The first case may be referred to as geographic gridding while the second case is a map projection grid.

Conceptually the geographic gridding is the simplest. Having obtained the transformation from ϕ, λ coordinates to x''', y''' coordinates using either equation (31) or (42) we pick a certain ϕ, λ as a starting point for the grid. Such values would probably be at some 1° intersection. Then we take all ϕ values and let λ vary. For each point we compute the x''', y''' coordinates. Connecting all such points we would obtain an image of some parallel (i.e. $\phi = \text{a constant}$). We may repeat, at some chosen interval, until the photo is completed with parallels. Then we start again holding the longitude constant varying the latitude. When the resulting x''', y''' coordinates

are computed we will have the image of a meridian. The computations are completed when the gridding of the photograph has been finished at the required interval.

5.2 The Height of the Grid

The photograph sees the actual terrain, not the points on the ellipsoid. Thus when constructing a grid to match the actual photograph, we should theoretically consider the elevation of each point on the photograph. One way to reduce the error of applying an ellipsoid grid to a photograph is to bring the grid to the mean height (\bar{H}) of the region. This may be done by using \bar{H} for all H_p in the equation (30) or its dependent equations.

The effect of this distortion may be visualized from Figure 8 where we see the image on the photograph of a point, once located on the ellipsoid and secondly located on the surface.

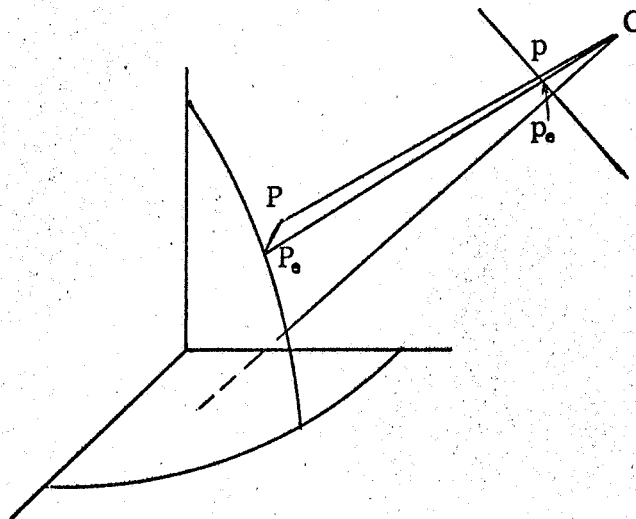


Figure 8

Effect of Elevated Point on Photograph

In figure 8 P_0 is the point on the ellipsoid corresponding to some point P on the surface. p_0 and p are the images of P_0 and P on the photograph. The

The error or distortion of assuming P is at P_0 would be the distance pp_0 .
Approximately we may write:

$$(43) \quad \overline{pp_0} \approx \frac{\overline{pn} \, dH}{H}$$

where \overline{pn} is the distance from the nadir point of the photo to the image on the photograph and dH is the difference in height between the reference surface and the terrain. If we assume that the gridding takes place at the mean elevation of the area, dH would be the difference between the mean elevation and the point elevation. Thus it can be seen that the effect of terrain height with respect to a mean height is small on a near vertical space photograph.

5.3 Gridding in a Specified Map Projection

We assume that it is desired to place on the photograph a grid corresponding to a particular map projection. Given the ability to convert a point given by its latitude and longitude into $x''' y'''$ the procedure is simple.

First it is necessary to define the map projection that will relate a given ϕ and λ on the reference ellipsoid to the X, Y coordinate of the projection. More important in this application is the conversion of an X, Y coordinate into latitude and longitude, a process commonly known as the inverse problem. Then ϕ and λ , corresponding to a certain X and Y is then converted to x''' and y''' and then plotted on the photograph. If we vary X leaving Y constant, solve the inverse problem for ϕ and λ each time, then convert to x''', y''' the connection of all such points will be an image of a certain constant Y coordinate. The process may be repeated at any desired interval. Then the whole procedure can be repeated for lines having a constant X . Thus it is possible to build up an image of the projection on the photograph.

It may be noted that although the X, Y axes on the map projection are

straight lines and orthogonal, they will not maintain such properties on the photograph.

5.31 Applications of the Universal Transverse Mercator (UTM) Projection

For non-polar areas the most widely used projection is the UTM. Full descriptions of this may be found in several publications, the most important of which is that published by the Army Map Service. We will discuss here only those equations of special interest to the gridding application.

The UTM is a Transverse Mercator type projection with a scale factor on the central meridian of 0.9996. The Y origin of the projection is at the equator in the Northern Hemisphere, with the X coordinate having a value of 500,000 meters on the central meridian. The world is divided into numbered zones, 1 to 60, so that the zone is 3° on each side of a central meridian. If n is the zone number, the central meridian, λ_0 of that zone would be: (λ positive east).

$$(44) \quad \lambda_0 = -6 (30 - n) + 3$$

We now outline the inverse problem for this projection. For this discussion we define the following terms:

a = equatorial radius of reference ellipsoid

e^2 = eccentricity, squared of reference ellipsoid

e'^2 = second eccentricity, squared

k_0 = scale factor on the central meridian (for UTM, $k_0 = 0.9996$)

$a' = ak_0$

$S\phi$ = scaled meridian distance from equator to latitude ϕ

ϕ, λ = geodetic latitude, and geodetic longitude with respect to longitude (λ_0) of central meridian

ϕ' = footpoint latitude (that latitude for which the scaled meridian distance is equal to the Y coordinate of the point)

X, Y = coordinates of projection

The scaled meridian arc from the equator to latitude φ

$$(45) \quad S\varphi = a' (1 - e^2) \left[A\varphi + \frac{B}{2} \sin 2\varphi + \frac{C}{4} \sin 4\varphi + \dots \right]$$

where:

$$A = 1 + \frac{3}{4} e^2 + \frac{45}{64} e^4 + \frac{175}{256} e^6 + \dots$$

$$B = \frac{3}{4} e^2 + \frac{15}{16} e^4 + \frac{525}{512} e^6 + \dots$$

$$C = \frac{15}{16} e^4 + \frac{105}{256} e^6 + \dots$$

$$D = \frac{356}{512} e^6 + \dots$$

Higher order terms may be found in Thomas. The steps in the inverse solution may now be formulated.

1. Compute the first approximation to φ' from:

$$(46) \quad \varphi_0' = \frac{Y_p}{a' (1 - e^2) A}$$

2. Compute $S\varphi$ for $\varphi_0' = \varphi_1'$. Then repeat solution for a better approximation to φ' :

$$(47) \quad \varphi_{i+1}' = \frac{Y_p - S(\varphi_i)}{a' (1 - e^2) A}$$

Repeat until there is no change, to accuracy required, in φ_{i+1}'

3. For φ' compute:

$$N = \frac{a'}{(1 - e^2 \sin^2 \varphi)^{\frac{1}{2}}}$$

4. Find:

$$(48) \quad \lambda = \sec \varphi' \left(\frac{X}{N} - \frac{1}{6} \left(\frac{X}{N} \right)^3 (1 + 2t_1^2 + \eta_1^2) + \frac{1}{120} \left(\frac{X}{N} \right)^5 (5 + 28t_1^2 + 24t_1^4 + 6\eta_1^2 + 8t_1^2 \eta_1^2) \right)$$

Then the actual longitude is $\lambda_p = \lambda + \lambda_0$

5. Compute the actual latitude of the point from:

$$(49) \quad \varphi = \varphi' - \frac{t_1}{2} (1 + \eta_1^2) \left(\frac{X}{N} \right)^2 + \frac{t_1}{24} (1 + \eta_1^2) (5 + 3t_1^2 + \eta_1^2 - 4\eta_1^4 + 9\eta_1^2 t_1^2) \left(\frac{X}{N} \right)^4 - \frac{t_1}{720} (61 + 90t_1^2 + 45t_1^4 + 107\eta_1^2 - 162e'^2 \sin^2 \varphi' + 45e' t_1^2 \sin^2 \varphi') \left(\frac{X}{N} \right)^6$$

In equations (48) and (49) we have:

$$t_1 = \tan \varphi'$$

$$\eta_1^2 = e'^2 \cos^2 \varphi'$$

These equations may be found in any standard map projection text (e.g. Thomas, 1952), or the Army Map Service Publication previously mentioned.

6. Results of Test Gridding

6.1 Introduction

In order to test the theories previously developed we were supplied, through the U. S. Geological Survey, several photographs taken during the flight of Gemini 11. These photographs were taken with hand held cameras. Because of this, the orientation of the camera was essentially unknown. In addition the exposure time was known only to the nearest minute, if that, and thus the location of the satellite could not be ascertained to the accuracy required for the application of the first described gridding method. However, method two; that is the surface fitting technique could be applied if sufficient control could be found on the photograph.

In addition to the photographs, which were in the Red Sea area, supplied to this contract were many maps at scales varying from 1: 50,000 to 1: 250,000. We supplemented these maps by the world navigation charts at the scale of 1: 1,000,000 produced by the Aeronautical Chart and Information Center.

The photographs themselves were supplied as color paper prints. Ideally we should use glass diapositives but we felt that for the test of the procedures, measurements made from these prints would be sufficient. In order to avoid marking on the color prints exact black and white copies were made. It was these later prints on which the actual measurements were made.

The general procedure was to identify various points on the photograph and on the map. As the photographs contained sea coast, identification was fairly easy for those parts of the photograph. However, it was difficult to find points in areas away from a coast line. This was for two primary reasons. 1) there were no prominent features and 2) the map portrayal was not complete in some areas. For example, one might think that bends in rivers could provide good control information. However, it was found that rivers on the map could look considerably different from the photograph. Thus in some cases it was difficult to establish a uniform density of control. In fact, most of the control that was used was obtained as coast line points.

After the control was identified, it was pin pricked on the photograph. The photograph was then placed on the Coordinatograph of the Wild A7 plotter. The x''' and y''' coordinates were then measured, usually twice for checking purposes. Then a preliminary surface fit was performed using equations (42). The residuals on x''' and y''' were then examined to point out any large residuals. Generally large residuals could be traced to misidentification of points on the photograph and the map. In some cases it was necessary to reject some control information due to reasons beyond our control, for example map inaccuracies.

In the following sections we describe the gridding results obtained from several photographs.

6.2 Photograph Number One

Photograph number one views parts of the Red Sea and the Gulf of Aden.

The ground control was obtained from the maps having a UTM grid system on them. The UTM coordinates were read from the map and converted to latitudes and longitudes using the inverse solution described in section 5.31.

We list in Table 1 the latitude, longitude, x''' , y''' values for the control selected for use in the gridding.

Table 1
Control Information Used in Photograph One

Point No.	ϕ°	λ°	$x'''(\text{mm})$	$y'''(\text{mm})$
1	11.5557	42.6831	74.886	140.864
2	11.5888	42.5136	80.153	143.447
3	11.47645	42.6996	73.355	143.779
5	11.3616	43.4821	48.676	128.479
6	11.35827	43.4900	43.324	134.182
7	10.39095	44.4428	6.108	140.399
8	11.98229	43.3716	65.539	113.708
9	12.46775	43.3284	76.843	99.716
10	12.83278	42.7935	99.836	98.649
11	13.0490	42.7279	106.938	93.263
12	13.19803	42.3836	120.552	94.448
13	13.63297	42.1220	138.563	86.487
14	13.86667	41.9400	149.347	81.775
15	14.11666	41.5583	168.345	81.246
16	14.40833	41.3300	181.144	76.271
17	15.66333	42.3000	175.001	22.864
18	15.62667	42.6367	163.854	19.034
19	15.30833	42.5417	161.170	29.279
20	14.91924	42.8934	142.095	35.088
21	14.42858	43.0277	127.963	46.917
24	13.61484	42.7178	118.839	76.181
25	13.30728	43.2318	97.577	77.390
26	12.83290	43.0751	91.812	93.067
27	12.67191	43.4670	77.703	90.981
28	12.60168	43.9182	64.556	85.279
29	12.66121	44.4203	53.381	74.992
30	12.78474	44.9728	43.094	63.380
32	13.34736	45.6594	39.239	39.476
33	13.42360	46.6767	19.877	24.636
34	13.63196	47.3480	11.748	11.677

Point number 13 was selected as the $\phi_0, \lambda_0, x_0''', y_0'''$, point leaving a total of 29 points for the adjustment. From the least squares adjustment the coefficients of equation (42) are given, along with the estimated standard errors, in Table 2.

Table 2
Coefficients of Equation. (42) For Photograph No. 1

	Coefficient	Standard Error		Coefficient	Standard Error
a_1	22.2862	± 0.310	b_1	-31.1870	± 0.243
a_2	-32.097	0.417	b_2	-18.2366	0.327
a_3	- 0.4237	0.125	b_3	0.4865	0.098
a_4	1.5010	0.097	b_4	0.7706	0.076
a_5	- 1.1601	0.298	b_5	1.8314	0.234

For the x''' coordinate fit the standard error of unit weight was $\pm 1.21\text{mm}$ while for the y''' coordinate fit the same quantity was $\pm 0.95\text{mm}$. We felt that this accuracy of approximately 1mm for fitting the measured coordinates demonstrated quite well the ability of the polynomial representation given in equation (42).

In this regard it is not only interesting to know how the x''', y''' residuals behave, but also what happens if we compute the value of ϕ and λ given the measured x''', y''' values, and compare the result with the measured ϕ and λ values. This may be done by an iterative solution of equation (43) until the ϕ and λ are found to yield, from the transformation using the least squares values of a_i and b_i , the exact measured coordinates. Taking the root mean square (RMS) difference between this ϕ and λ and the known values we found the RMS difference for the latitude was ± 0.035 and ± 0.036 for the longitude.

The gridding was then carried out according to the procedures previously described. The geographic grid is shown in Figure 9. Mechanically the grid was made by superimposing the created grid over the original color photograph and photographing the results. This procedure is not ideal and if a quantity of photographs were to be gridded, a more sophisticated procedure should be used.

This photograph is also shown in Figure 10 with the UTM grid for zone 38 imposed on it. It may be noted that the X coordinate is negative toward the lower left-hand edge of the photograph. Generally the UTM would change zones before the X coordinate became negative; however, it was felt that to have two UTM zones on the photograph could be confusing. With this photograph the problem is not too great, but with a photograph that fell centrally on an area near the edge of two UTM zones it may be required to portray two different UTM grids.

6.3 Photograph Number 2

This photograph shows part of the Red Sea, Egypt, Israel, and a portion of the Mediterranean Sea. By inspection we can see that there is a fairly large tilt to the photograph. Points were identified along coast lines and on the Nile River. The data that was actually used in these tests is given in Table 3.

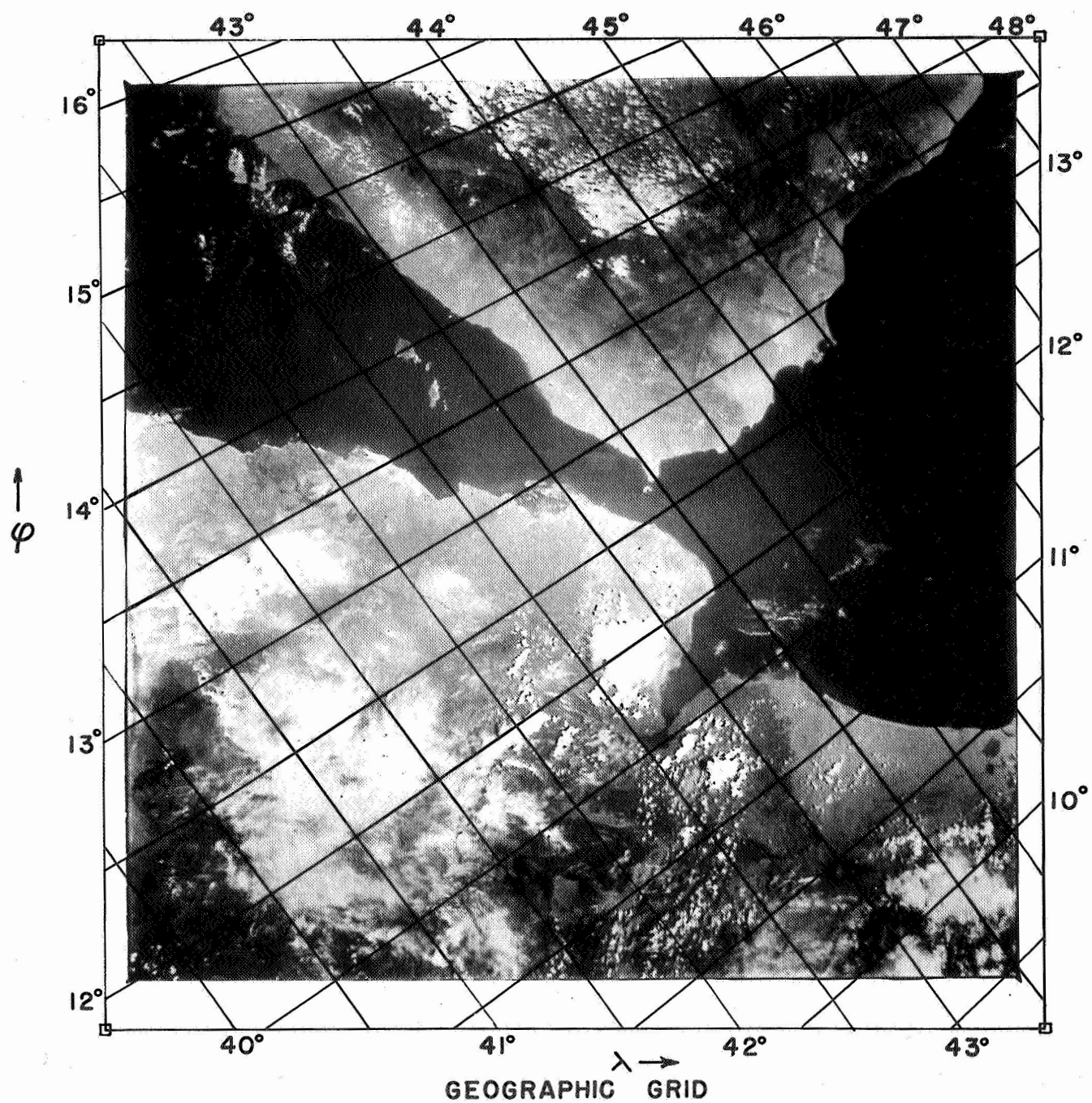


Figure 9

Geographic Grid of Photograph No. One

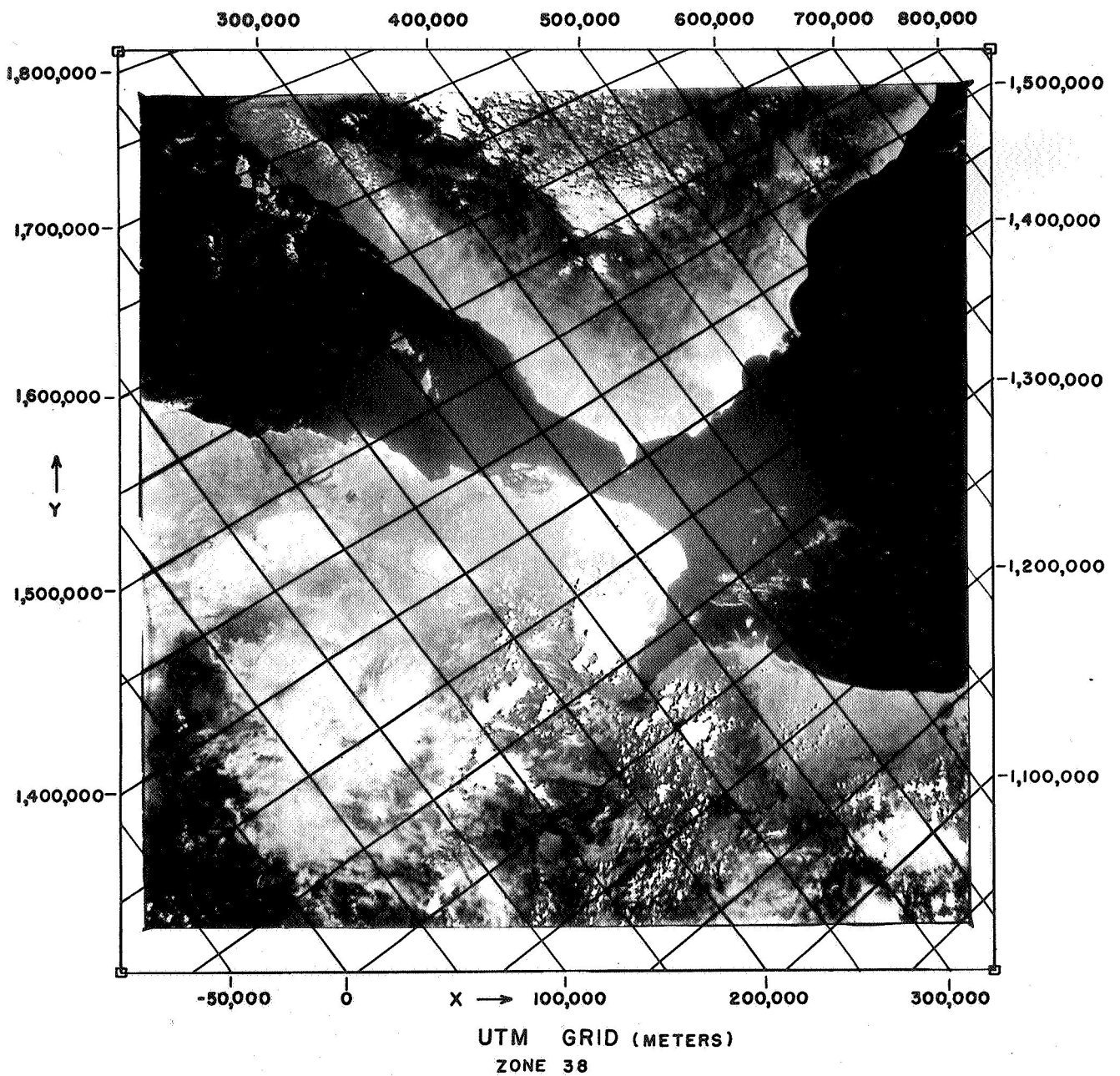


Figure 10

UTM Grid of Photograph No. One

Table 3
Control Information Used in Photograph Two

Point No.	ϕ°	λ°	$x'''(\text{mm})$	$y'''(\text{mm})$
4*	24.3267	35.3833	96.069	43.112
6	25.9667	34.3667	53.472	70.879
7	26.7000	34.0000	39.457	82.352
8	27.6367	33.5917	25.681	96.323
9	28.0833	33.3333	18.905	101.862
10	27.7200	34.2417	36.065	105.710
11	28.0867	34.5783	38.578	116.140
12	28.6700	40.7800	38.796	128.058
13	29.5467	34.9533	34.863	143.291
14	31.3500	35.5000	32.458	170.839
15	27.7867	35.3483	54.432	120.330
16	27.0750	35.7483	69.311	112.572
17	26.7500	36.0767	78.855	109.993
18	26.1550	36.4300	97.957	102.572
20	24.8400	37.1167	128.436	82.431
21	24.2683	37.6000	151.588	75.078
23	23.5333	38.5533	179.054	75.443
24	23.0433	38.7833	188.858	70.427
28*	26.0983	32.7400	21.457	53.834

* not used in final computations; see text.

Using this data and with point 17 as a center the surface fitting was carried out. For the x''' coordinate the standard error of unit weight was $\pm 4.46\text{mm}$, with $\pm 3.72\text{mm}$ for the y''' coordinate. However, it was noted that the residuals on points 4 and 28 were quite large. For point 4, the residual of x''' and y''' was 7.5mm and 6.2mm respectively; for point 28 the similar residuals were -7.5mm and -7.5mm . The reason for the large residuals is not clear at this time. Point 28 was located on the Nile River which was well defined in the photograph and map so that it would be expected to be good. One possible explanation is that the map that was used in this area is wrong, or perhaps the river has shifted its course since the map was made.

The adjustment was then repeated deleting points 4 and 28. In this

computation the standard error of unit weight was $\pm 3.15\text{mm}$ for x''' and ± 2.10 for y''' . The largest residual in x''' was 4.8mm and in y''' 4.3mm .

The constants obtained from this adjustment are given in Table 4.

Table 4
Coefficients of Equation (43) For Photograph No. 2

	Coefficient	Standard Error		Coefficient	Standard Error
a_1	-14.7453	± 0.939	b_1	17.9990	± 0.625
a_2	13.4650	0.962	b_2	10.0622	0.640
a_3	1.0183	0.287	b_3	- 1.1050	0.191
a_4	- 2.4342	0.151	b_4	- 1.6728	0.100
a_5	- 2.7472	0.519	b_5	- 2.4859	0.345

The geographic grid obtained from these constants is shown in Figure 11. The convergence of the meridians and parallels testifies to the tilt of the photograph. No grid is shown for the upper right portion of the photograph as no control was used from this area and thus the constants of Table 4 do not yield meaningful results for this area. The accuracy of the grid, where it exists is best in the region where control was used. Thus the reliability of the grid toward the bottom of the photograph could be $\pm 30'$ or somewhat poorer. In the area of control, it is probably on the order of ± 5 to $10'$ or somewhat better. This grid points out the limitations of using control in certain areas, and not in the others. Sometimes one may obtain a smooth, but not highly accurate grid, as in the left bottom of the picture, while other times we will not be able to generate a grid at all. This latter feature occurs toward the top of the photograph.

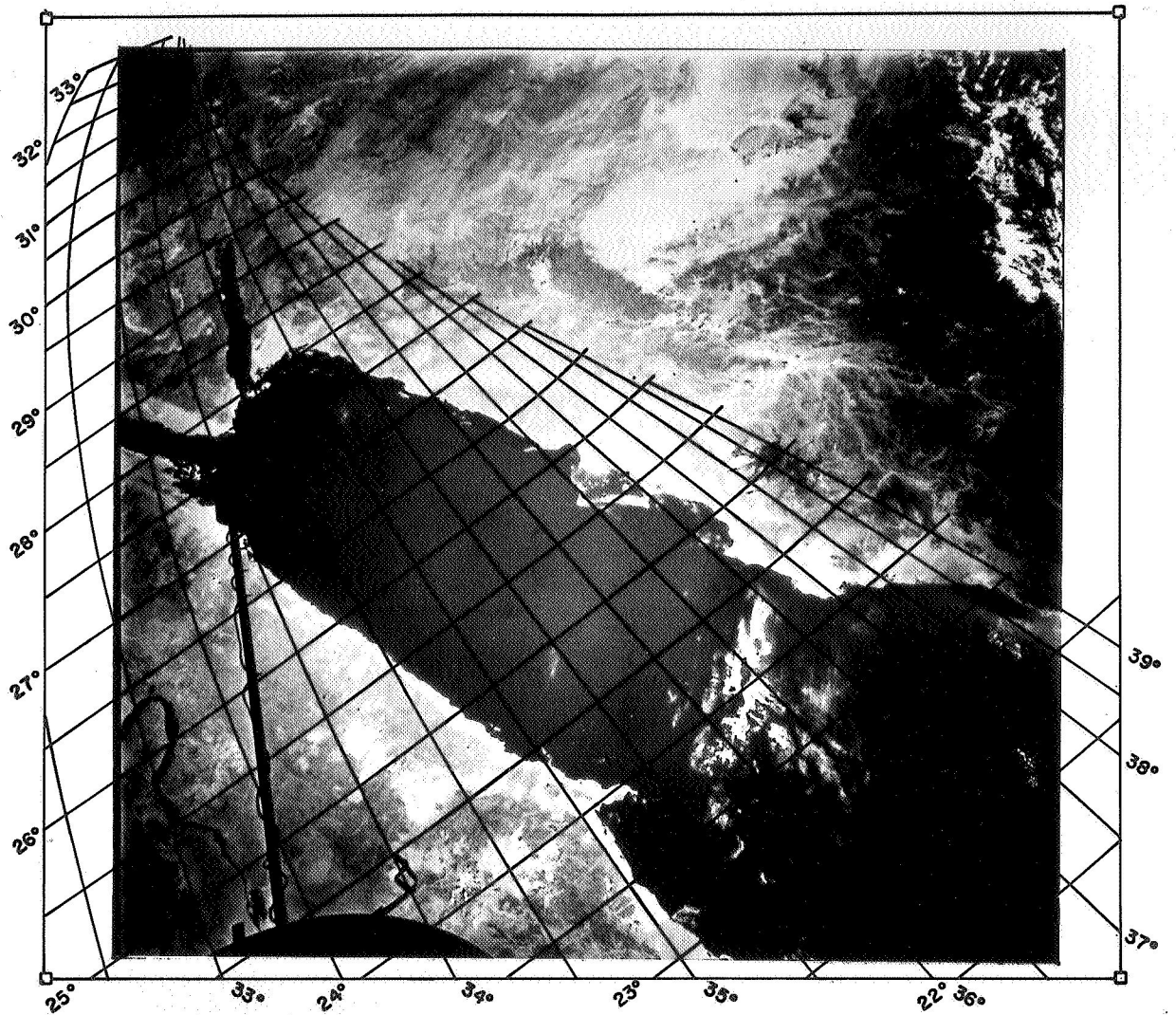


Figure 11

Geographic Grid of Photograph No. Two

6.4 Photograph Number Three

This photograph is in the same area as the first photograph. Twenty-four control points were obtained from the ACIC maps at the scale 1: 1,000,000. The data used in the surface fitting for this photograph is shown in Table 5.

Table 5

Control Information Used In Photograph Three

Point No.	ϕ°	λ°	$x'''(\text{mm})$	$y'''(\text{mm})$
1	15.5500	40.4167	32.673	89.309
2	14.6167	41.1767	48.243	85.186
3	13.8333	41.9667	61.852	82.514
4	13.2333	42.5333	77.938	80.684
5	11.9833	43.3633	102.250	71.463
6	11.3667	43.4917	111.192	64.399
7	10.4333	44.7500	141.268	63.710
8	10.6333	45.3100	146.220	73.949
9	10.8750	45.7833	149.885	82.382
10	11.1667	47.4167	166.462	102.972
11	11.2250	48.3000	176.456	111.982
12	11.3250	49.3000	185.875	121.973
13	15.5500	52.2600	162.255	173.282
14	14.8250	49.9667	151.371	157.411
15	13.9833	48.4533	144.632	140.683
16	13.6417	47.3833	136.614	129.969
17	13.3500	43.6500	118.710	112.297
18	12.7750	44.9750	115.890	99.294
19	12.6833	43.4583	96.102	82.818
20	13.2917	43.2167	87.105	88.303
21	14.5250	42.9500	73.411	100.589
22	15.7217	42.6917	60.585	111.312
23	17.0200	42.3583	48.937	121.795
24	18.5833	41.2867	29.790	125.578

Point number 19 was chosen as the reference point (i.e. that point whose coordinates are $\phi_0, \lambda_0, x_0''', y_0'''$). The least squares adjustment was then carried out with 23 points. From this adjustment the coefficients of equation (42) and their estimated standard errors are given in Table 6.

Table 6

Coefficients of Equation (43) For Photograph No. 3

	Coefficient	Standard Error		Coefficient	Standard Error
a_1	-10.0460	± 0.230	b_1	13.5295	± 0.068
a_2	13.7676	0.170	b_2	10.3224	0.050
a_3	0.5257	0.053	b_3	-0.6470	0.016
a_4	- 0.2229	0.025	b_4	-0.2047	0.007
a_5	- 0.4992	0.046	b_5	-0.7171	0.014

For the x''' coordinate fit the standard error of unit weight was $\pm 1.14\text{mm}$ while for the y''' coordinate the unit weight standard error was $\pm 0.340\text{mm}$.

The latter figure indicated the best fit for any photograph tried in these tests.

The photograph and its grid are shown in Figure 12. No grid was drawn for the top of the photograph as the image of the parallels were becoming very closely space. It may also be noticed that toward the right top edge there appears to be a small area where several meridians and parallels appear to converge. The cause of these two facts is that no control was available toward the top of the photograph. As previously mentioned and described, this gridding method may only yield satisfactory results in areas where control is present. As with the other two grids, the best accuracy of the grid would be in the area of the existing control. However, this statement must be tempered by the fact that the photograph - map identification of the control points is not perfect. Thus we can not rely 100% on the accuracy of the control.

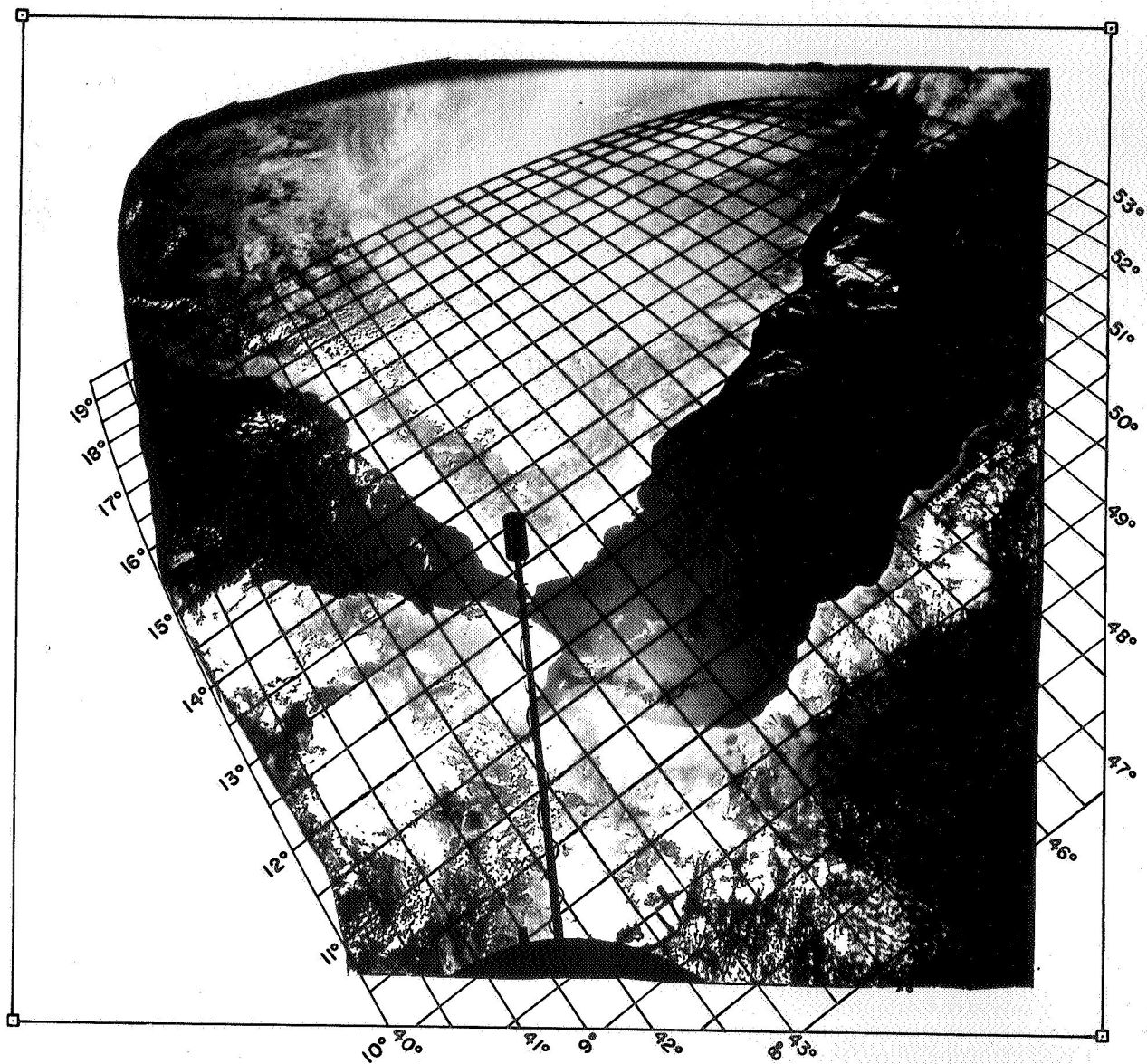


Figure 12

Geographic Grid of Photograph No. Three

7. Discussion and Conclusion

7.1 Summary

The purpose of this report has been to show the mathematical basis for the relationships between points on a space photograph and points on the surface of the earth, taken as an ellipsoid of revolution, and to demonstrate some actual gridding procedures.

We found that the rigorous method required approximate values for the location and orientation of the space photograph. Such parameters are not generally available today for the type photograph being made from the Gemini spacecraft. Thus there was a need to develop the surface fitting procedure that used control points on the ground, in conjunction with the measured coordinates on the photograph. Several photographs were gridded by this technique. The problem is that this method works best with a good distribution of control and when the photograph is not far from being vertical.

7.2 Conclusion

The gridding of a space photograph enables such a picture to become a map. How accurate a map will depend on many factors, such as the accuracy of the location and orientation of the camera, the ground control, camera distortion, etc.

Once the proper relationship is found between the coordinates on the surface of the earth and the coordinates on the photograph, any type grid may be constructed. The most obvious one is the geographic gridding in terms of latitude and longitude. Then we can adopt some particular map projection. This could be a conformed type projection, such as the Universal Transverse Mercator or a Lambert Conformal Conic. However it should be noted that this procedure will only give an image of the grid lines and of the specified projection, on a given photograph. It does not make a conformal map out of the photograph.

The use of ground control deserves further explanation. Ideally we would like to take a photograph, place a grid on it and then use it as a map. In order to do this we must have some location and orientation information. This could take several forms: 1) Somehow a technique is found to give a precise definition to the location and orientation of the camera taking the photograph. How precise these parameters will be needed will depend on the accuracy requirements for the gridding of the photograph. 2) We only know approximate values for location and orientation parameters; however, in addition we have some ground control. Then an adjustment procedure, as described in this text (for near vertical photographs) should be carried out. 3) Only ground control information is available. Then the surface fitting technique must be carried out.

The first situation is an ideal one. If it were to work, then it would be possible to construct maps of completely unsurveyed areas. The other two procedures are less desirable as we would need to have maps or at least control, in the area being considered.

7.3 Future Work

This report has brought out several questions that should be answered, and procedures that should be developed. Among these are the following:

1. Formulation of a computer program to carry out the adjustment procedure described in this report. Such a program should be able to take all input parameters, such as the location and orientation of the photograph, control data, refraction models, camera distortions etc. In addition, tests should be made to determine how accurately the approximate values are required. This in turn could be related to how accurately should we record the time the photograph was taken.

2. Develop the system analogous to that in this report for photographs for which the assumption of near vertical is not made. Thus we would attempt

a general system for tilted photographs.

3. Investigate the refraction and camera distortion effects on the gridding.

4. If we do not consider any ground control, how accurately do we need to determine the location and orientation of the spacecraft for various accuracies in the gridding.

5. Consider an application of analytical photogrammetric equations to the mathematics and adjustment using space photographs.

References

- Bonner, W. D., A Program For Computer Gridding of Satellite Photographs For Mesoscale Research, SMRP Research Paper, No. 43, June 1965, Department of the Geophysical Sciences, The University of Chicago.
- Dumitrescu, V., Cosomographic Perspectives - A Useful System of Azimuthal Projections, Roumanian Geology, Geophysics and Geography, Series of Geographie, Vol. 10, No. 1, 1966.
- Dumitrescu, V., Construction of Perspective Space Projections, Roumanian Geology, Geophysics and Geography, Series of Geographie, 1967.
- Fujita, T. , A Technique For Precise Analysis of Satellite Photographs, Research Paper No. 17, Department of the Geophysical Sciences, The University of Chicago, April, 1963.
- Fujita, T. , Evaluation of Errors in the Graphical Rectification of Satellite Photographs, J: Geophysical Research, Vol. 20, No. 24, Dec. 15, 1965.
- Grenard, H. E. , ARACON Gridding Program for the CDC 160-A Computer Configuration, Program Documentation, Technical Report No. 2, Contract No. NAS 5-1204, ARACON Geophysics Co., 1963.
- Robbins, A., Long Lines On the Spheroid, Empire Survey Review, April, 1962.
- Schmid, H., and Schmid, E., Generalized Least Squares Solution for Hybrid Measuring Systems, The Canadian Surveyor, 1965.
- Thomas, P. D., Conformal Projections in Geodesy and Cartography, U.S. Coast and Geodetic Survey, Special Publication No. 251, 1952.
- Universal Transverse Mercator Grid, 1958, Department of the Army Technical Manual TM 5-241-8
- Widger, W. Jr., Orbits, Altitude, Viewing Geometry, Coverage, and Resolution Pertinent to Satellite Observations of the Earth and Its Atmosphere, ARACON Geophysics Division, Allied Research Associates, Inc., Concord, Mass.